

OPTIMISATION OF AN INVERSE COMPTON SCATTERING EXPERIMENT WITH A REAL TIME DETECTION SCHEME BASED ON A RADIO LUMINESCENT SCREEN AND COMPARISON OF THE X-RAYS BEAM CHARACTERISTICS WITH SIMULATIONS

A.-S. Chauchat[#], J.-P. Brasile, THALES Communications and Security, Colombes, France,
V. Le Flanchec, J.-P. Nègre, A. Binet, CEA DAM DIF, Arpajon, France, J.-M. Ortega, CLIO/LCP,
Université Paris-Sud, Orsay, France

Abstract

To optimize the detection of an 11 keV X-ray beam produced by Inverse Compton Scattering at the ELSA facility, with a 17 MeV electron beam and a 532 nm laser, we demonstrate the use of a very sensitive detection scheme, based on a radio luminescent screen (imaging plate) used in the spontaneous emission regime. It has proven to be very sensitive and very effective to detect 11 keV X-rays while rejecting the overall ambient noise produced in a harder spectral range. It allowed us to optimize the electron-photon interaction probability by observing in real time the effect of both beams transport parameters. We could then compare simulation results with experimental measurements that appear to be in good agreement.

INTRODUCTION

The X-ray Compton source under development at the ELSA facility, is designed to be an experimental proof of principle of this type of compact sources for applications such as cultural heritage, medical imaging, cancer therapy, but also a calibration tool to study the response of fast detectors like X-streak cameras and integral imagery cameras. It delivered its very first photons at 11 keV in August 2009, which were detected with radioluminescent imaging plates. These plates allowed us to show the image of the beam transverse profile [1]. Generally, exposed imaging plates are read by a scanner. This process takes several minutes, which forbids its use in real time for an optimization process. Several detection schemes were tested and didn't give exploitable results for such an optimization because of a too-low sensitivity and a bad signal-to-noise ratio. Therefore we tested the idea of using our radioluminescent plates in the spontaneous emission regime, i.e. by directly detecting the emitted visible photons with a photomultiplier tube.

RADIOLUMINESCENT PLATES

The Imaging Plates (IP) we use consist of a flexible plastic substrate covered by a 115 μm thick layer of $\text{BaF}(\text{Br,I})\text{Eu}^{2+}$ radiosensible crystals combined in an organic binder, with a 10 μm thick transparent protection plastic film. Fig. 1 depicts the radioluminescence process.

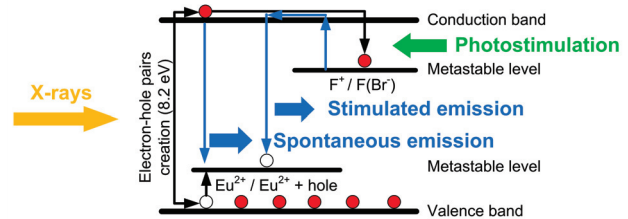


Figure 1: Mechanism of PSL in $\text{BaF}(\text{Br,I})\text{Eu}^{2+}$

Stimulated Emission

Radioluminescent IP, through the photostimulated emission, are generally used in conjunction with a separate excitation optical unit (scanning system). The energy trapped in the metastable sites is released thanks to a photostimulation process by a 633 nm laser. PhotoStimulated Luminescence (PSL) is converted to a numeric signal by a photomultiplier and an A/D converter. This technique was used in our previous paper [1].

Spontaneous Emission

As shown in the diagram, Fig. 1, spontaneous emission also occurs under X-ray radiation. This emission is almost simultaneous to the excitation process and is based on the part of the energy that never reaches the metastable level. Such as the photostimulated emission, the spontaneous luminescence is emitted by the 5d-4f Eu^{2+} transition at 390 nm (3.2 eV). To observe this visible signal on an oscilloscope, we couple the radioluminescent IP with a photomultiplier tube (PMT) (Fig. 2).

A small piece of a radioluminescent imaging plate ($\sim 50 \times 40 \text{ mm}^2$) is placed at a 45° angle on the X-ray beam axis. The photocathode of the PMT faces the plate, also at a 45° angle. A thin aluminium foil (50 μm) is placed before the plate to get rid of parasitic light (Fig. 2). One major interest of this radiator lies in the fact that it is very sensitive in the 1-100 keV spectral range thanks to its thickness while it is much weaker in the 1-10 MeV region, which is typically where we have the more annoying noise, originating from Bremsstrahlung X-rays production of the electron beam halo on the accelerator tubes and residual particles. That is the reason why we could not efficiently observe any useful signal with other radiators or other detectors, like solid-state detectors.

[#]anne-sophie.chauchat@thalesgroup.com

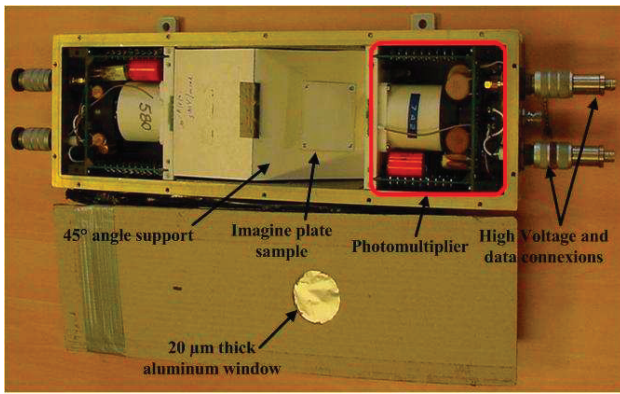


Figure 2: Photograph of the real-time detector made by coupling between the imaging plate and the photomultiplier tube.

EXPERIMENTAL RESULTS

The experimental setup was detailed in reference [1], along with some theoretical aspects of the Compton Scattering process. The electron beam of the ELSA accelerator [2] is produced from a photo-injector upstream of a radio-frequency accelerator at 433 MHz. The kinetic energy of the 12.7 ps electron bunches after acceleration is 17 MeV. The 532 nm photons are obtained by frequency doubling 1064 nm photons out of a Master Oscillator Power Amplifier (MOPA) system based on a mode-locked Nd:YVO₄ oscillator and on a flashlamp-pumped Nd:YAG amplifier chain. The optical pulses width is the same as the electron pulses one.

Typical signals provided by the real-time detector are shown in Fig. 3. When the laser involved in the interaction is off, the background noise is observed, due to high energy Bremstrahlung photons. When it is turned on, 11 keV X-rays produced by interaction are more efficiently absorbed in the thin imaging plate phosphor layer which produce a peak of luminescence light.

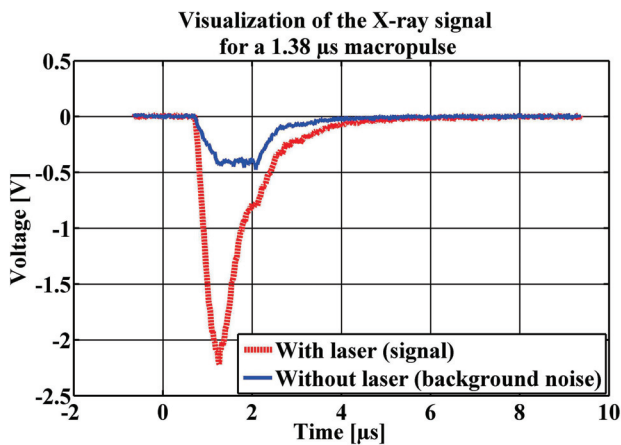


Figure 3: Observation of X-rays signal by the real-time detector.

Observing these signals in real time allowed us to optimize the interaction. It was done by slightly adjusting the electron beam direction with steering magnets, and by adjusting the time delay between the electron and photon pulses. The typical signal-to-noise ratio obtained after optimization is 5.5.

One key-optimization lies in the minimization of the ambient noise. The electron beam transport prior to the final focusing has to be optimized to avoid Bremsstrahlung X-rays production by its halo. Therefore, we alternately switched the laser on and off to monitor both signal and noise. The interaction parameters measured after the optimization of the signal are listed in table 1.

Table 1: Interaction Parameters after Signal Optimization

Macropulse width	1.38 μ s @ 1 Hz
Pulse width	12.7 ps [rms] @ 72 MHz
Electron pulse charge	0.24 nC
Laser pulse energy	0.7 mJ
Electron beam sizes at interaction point	70 μ m [rms] horizontal 50 μ m [rms] vertical
Electron beam normalized emittance	30 μ m.rad [rms] horizontal 20 μ m.rad [rms] vertical
Laser beam size at interaction point	60 μ m [rms]
Collision angle	30 mrad
Irradiation duration	120 s

We noticed that the minimization of the background noise is not necessarily reached with the same transport as the one obtained for the emittance minimization. There might be a trade-off between the two situations, because minimizing the emittance growth inside ELSA U-turn [2] leads to have quite large diameter beam in the second branch of the U, which, in turn, widens the beam halo. This explains the fact that best results were not detected with the best measured emittance.

Optimizing the interaction thanks to real time detection, allows us to observe an intense profile in a digital image, compared to the background noise (Fig. 4).

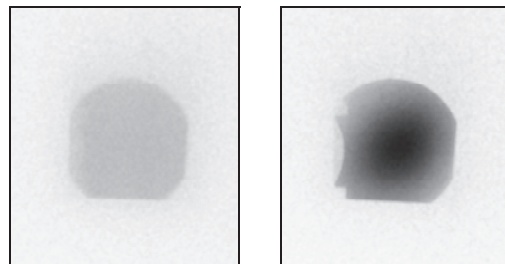


Figure 4: Visualization of the signal observed on an photostimulated imaging plate, without laser on the left picture, with laser on the right picture.

CHARACTERIZATION OF THE EMISSION CONE

Profile

Theoretically, X-rays emission cone size is given through the half angle of the emission cone by :

$$\theta \approx \frac{1}{\gamma} \quad (1)$$

in the case of ideal beams (i.e. for a 17 MeV electron beam, relativistic factor $\gamma = 34$, $\theta = 29$ mrad). For real beams (Gaussian shaped) electron beam and laser beam bring their own contribution to the X-ray beam divergence. In the case of our experiment, the most valuable contribution is the one from the electron beam divergence because of the non-negligible emittance of our electron beam.

In Fig. 4, we observe first of all that the X-ray beam profile is oriented at 45° clockwise. This orientation is related with the laser beam polarization. It can be explained if one considers the Compton scattering as a Thomson scattering effect in the electron frame: in this case, the vibration of the electron produces the so-called "dipole" radiation, which is non-existent on the axis of the vibration, and maximum in the plan perpendicular to the vibration. In our experiment, the angle of the laser polarization was a little less than $\pi/4$ rad. Fig. 4 confirms that there is conservation of the polarization between the incident laser and the produced X-ray beam. Elliptic shape of the X-ray beam profile is mainly due to both electron beam emittance and laser polarization. This aspect of Compton scattering is correctly taken into account in CAIN simulation [3].

Quantification

As the sensitivity of a pixel (in PSL unit/X-ray photon) is given as a function of X-ray energy, we need to know the relation between a pixel position and photons mean energy of this pixel. In order to have accurate results we use simulation to know approximately the energy of each pixel. Adding, over a certain angle, the number of photons of each pixel, we have a good estimate of the X-rays emission flux.

The number of photons obtained with the parameters of Table 1 is summed up in Table 2.

Table 2: Experimental Results

Half angle of the emission cone	10 mrad
Number of X-ray photons for a pulse	120
Peak flux [X-ray photons/s]	$4.5 \cdot 10^{12}$
Average flux [X-ray photons/s]	$1.2 \cdot 10^4$
Peak surface flux [X-ray photons/s/cm ²]	$1.5 \cdot 10^{12}$

Extrapolating these results to the whole emission cone, we can estimate the total number of emitted X-ray photons to $1.8 \cdot 10^3$ photons by pulse. The calculation proceeded for ideal beams gives a total number of photons close to $3 \cdot 10^3$. Thus, we can evaluate to around

60 % the interaction yield between beams with parameters listed in Table 1.

Energy

To evaluate the X-ray beam energy, we use an image plates stack and deduce energy from the X-rays attenuation through the different layers. Comparing the radiation transmission through each plate with simulations done by MCNP code, we find that the extracted from noise X-ray signal energy is lower than 15 keV which is consistent with calculations (Fig. 5).

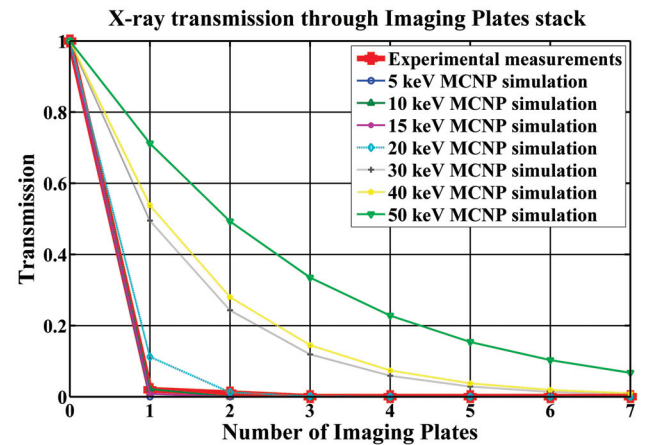


Figure 5: X-ray signal transmission through a stack of imaging plates, comparison between experimental and simulated results.

CONCLUSION

In this paper we show that imaging plates were the best way to observe Compton X-ray signal in our experiment. The use of these plates coupled with a photomultiplier lets us to optimize the interaction yield in real time. This improvement of our detection system gave us a signal over noise ratio sufficient to observe the influence of laser polarization and electron beam emittance on the X-ray beam cone. We were able to compare experimental X-ray cone size with simulation. The number of emitted photons is consistent with simulation. A stack of imaging plates can give an evaluation of the X-ray beam energy.

REFERENCES

- [1] A.-S. Chauchat, et al. Instrumentation developments for production and characterisation of Inverse Compton Scattering X-rays and first results with a 17MeV electron beam, NIMA Vol. 622, Pages 120-135, 2010
- [2] J.-G. Marmouget et al., Present performance of the low-emittance high bunch charge ELSA photo-injected linac, Proceedings of EPAC 2002, Paris, France.
- [3] K. Yokoya and P. Chen, User's manual of CAIN, <http://lcdev.kek.jp/~yokoya/CAIN/cain235/>